

Steam Reforming of Alcohols for Hydrogen Production

Ivana Buffoni, Gerardo Santori, Francisco Pompeo and Nora Nichio*

Facultad de Ingeniería, PIDCAT, Universidad Nacional de La Plata, 1 esq. 47, 1900, La Plata, Argentina. CINDECA, Facultad de Ciencias Exactas, Universidad Nacional de La Plata. CCT La Plata-CONICET, 47 N° 257, 1900, La Plata, Argentina

Abstract: To understand the complexity of the reactions involved in the steam reforming of glycerol and with the aim of identifying the contribution of C-C and C-O bonds cleavage, in this work we have studied the steam reforming of C3 alcohols simpler than glycerol such as 1-propanol, 2-propanol, 1,2-propanediol and 1,3-propanediol. A Pt/SiO₂ catalyst was employed and were studied the conversion and the product distribution for each alcohol. It was possible to determine the absence of C-O and C-C bonds cleavage in a secondary alcohol such as 2-propanol and 1,2 propanediol. The presence of reaction intermediates with an aldehyde function, deactivates the catalyst due to their strong adsorption on the metal site, moreover, the presence of hydroxyl-aldehydes promotes the C-C bonds cleavage favoring the gas production. The reaction pathway from glycerol to acetol by cleavage C-O bonding or dehydration on metal site is responsible for the subsequent reactions leading to deactivation.

The main reaction pathway to obtain gaseous products from glycerol reforming involve C-C bonds cleavage of primary alcohols such as 2,3-dihydroxypropanal, 1,2-ethanediol and 2-hydroxyethanal. In order to confirm the proposed reaction pathways, steam reforming of ethylene glycol was performed, identifying this compound as primary intermediates to obtain gaseous products from glycerol.

Keywords: C3-alcohols, platinum catalyst, steam reforming, hydrogen production.

1. INTRODUCTION

Increasing fossil fuel prices because of limited reservoirs and the increase in the atmospheric CO₂ concentration owing to fossil fuel consumption have stimulated a greater interest in biomass utilization for sustainable production of energy and chemicals. The developments of new technologies for biomass valorization raise therefore great interest.

Among these alternatives, the production of hydrogen from steam reforming in gas phase products from biomass, appears as a promising alternative.

In this sense, the interest on the conversion of biomass to hydrogen has increased considerably during the last years. Among the various renewable feedstock sources (methanol, ethanol, polyols) glycerol is one alternative because it has a relatively high hydrogen content, it is non toxic, and its storage and handling is safe [1, 2].

In glycerol steam reforming several studies has been performed. High H₂ productions and glycerol conversions have been observed using Ru/Y₂O₃ at 600 °C [3], Ir/CeO₂ at 400°C [4], and Ni and Rh supported catalysts at 900°C [5, 6].

In previous works, we have studied different platinum catalysts prepared by different methods and using various supports such as SiO₂, γ -Al₂O₃, ZrO₂, CeO₂-ZrO₂, which

were active in the range of 350-450°C. Materials with acid properties (γ -Al₂O₃, ZrO₂, CeO₂-ZrO₂) demonstrated low activity to gaseous products, with formation of lateral products due to dehydration and condensation reactions, which would lead to coke formation and to a fast catalyst deactivation.

On the contrary, the catalyst prepared with a support with neutral properties such as SiO₂ permitted to obtain a catalyst with excellent activity levels to gaseous products, high selectivity to H₂, and a very well stability in time [8, 9].

However, the formation of carbon deposits and deactivation of the catalysts remain as an unsolved problem [7]. Therefore, a catalyst that promotes carbon deposit gasification and that will be active for the water gas shift reaction (WGS) is required to preserve the initial activity of the catalyst.

To understand the complexity of the reactions involved in the steam reforming of glycerol and with the aim of identifying the contribution of C-C and C-O bonds cleavage, in this work we have studied the steam reforming of 1-propanol, 2-propanol, 1,2-propanediol and 1,3-propanediol to understand the catalytic chemistry of C3 alcohols simpler than glycerol. Besides, the catalyst system employed, the production of H₂ from other alcohols could be affected by the number and position of the OH groups in the carbon chain and also the occurrence of reactions of dehydration/hydrogenation [10]. Furthermore, with the aim of confirming the proposed reaction pathways for glycerol reforming, ethylene glycol (1,2-ethanediol) and acetol (2,3-dihydroxypropanal) reforming was performed.

*Address correspondence to this author at the Facultad de Ingeniería, PIDCAT, Universidad Nacional de La Plata, 1 esq. 47, 1900, La Plata, Argentina. CINDECA, Facultad de Ciencias Exactas, Universidad Nacional de La Plata. CCT La Plata-CONICET, 47 N° 257, 1900, La Plata, Argentina; Tel: 00 54 221 4210711; Fax: 00 54 221 4254277; E-mail: nnichio@quimica.unlp.edu.ar

2. EXPERIMENTAL SECTION

Platinum catalyst was prepared at room temperature by ionic exchange method, with an aqueous solution of $[\text{Pt}(\text{NH}_3)_4]\text{Cl}_2$. A Degussa silica (Aerosil 200, $200 \text{ m}^2 \text{ g}^{-1}$) was employed as support. The ionic exchange isotherms of Pt on SiO_2 were performed in order to determine the maximum exchange capacity of the support with each precursor. The maximum metal content obtained was 2 %wt for Pt.

The specific surface areas were measured using nitrogen adsorption equipment Micromeritics Accusorb 2100E. The experiments were conducted at -196°C , employing 200 mg of sample previously degassed at 200°C under vacuum for 2 h.

Temperature programmed reduction tests (TPR) were carried out in a conventional dynamic equipment, with a H_2/N_2 ratio of 1/9 and heating rate 10°min^{-1} from room temperature up to 1000°C . Hydrogen chemisorption measurements were carried out in dynamic equipment with a TCD detector. Sample was reduced in H_2 at 500°C during 1h, cooled in H_2 up to 400°C , flushed with Ar for 2 h at 400°C and then cooled up to room temperature in Ar flow. Hydrogen pulses were then injected up to saturation. Dispersions were estimated from the hydrogen amount consumed, assuming an adsorption stoichiometry $\text{H}/\text{Pt}=1$.

Mean particle size was determined by TEM and obtained in a TEM JEOL 100 C instrument. A graphite pattern was used for calibration. In order to estimate the average particle size, the particles were considered spherical and the diameter volume-area was calculated by using the following expression $d_{va} = \frac{\sum ni \cdot di^3}{\sum ni \cdot di^2}$, where ni is the number of particles with diameter di .

The XPS analysis was carried out in a multi-technique system (Specs), equipped with a dual Mg/Al X-ray source and a hemispherical PHOIBOS 150 analyzer operating in the fixed analyzer transmission (FAT) mode. The spectra were obtained with a pass energy of 30 eV and an Al-K α anode operated at 200 W. The pressure during the measurement was less than 2.10×10^{-8} mbar. The samples were subjected to a reduction during 10 minutes at 500°C in H_2 5%/Ar flux in the pretreatment chamber of the equipment. The binding energy (BE) of the C 1s peak at 284.6 eV was taken as an internal standard. The intensities were estimated by calculating the integral of each peak after subtraction of the S-shaped background and fitting the experimental peak to a Lorentzian/Gaussian mix of variable proportion.

The experimental equipment used for reaction tests of alcohols reforming is a fixed-bed quartz reactor (8 mm internal diameter) operated isothermally at atmospheric pressure. The Pt catalyst was reduced from room temperature up to 500°C (10°min^{-1}) for 1 hour in H_2 flow ($30 \text{ cm}^3 \text{ min}^{-1}$). The aqueous solution of alcohols (10% wt) was injected to the reactor by a HPLC pump (Waters 590) with feed flow $0.5 \text{ cm}^3 \text{ min}^{-1}$. The evaporator is a stainless steel tube of 6 mm diameter filled with quartz pellets heated by an electric furnace. The nitrogen was used as carrier gas ($50 \text{ cm}^3 \text{ min}^{-1}$). The space time (τ = min) is defined as WHSV^{-1} , where WHSV was calculated as grams of feed per minute (N_2 , H_2O and alco-

hols) per grams of catalyst. The space time used in this study was from 0.88 min. The equipment has two sampling ports, which allows analyzing the liquid products of the collecting flask and gaseous products. The analysis of gaseous products was performed with a gas chromatograph Shimadzu GC-8A equipped with a column HayeSep DB 110-120 and GC/TCD detector. The liquid products were analyzed by gas chromatography with GC/FID (Chrompack) and mass spectrometry CG/MS detector (Shimadzu GCMS-QP5050A) with HP-PONA capillary column (50 m). The accuracy of the measured values was within 5% and the experiments could be reproduced with a relative error of 10%.

The alcohols conversion to gaseous products (CO , H_2 , CO_2 and CH_4) is indicated as X_G and it was calculated based on the following equation:

$$X_G = \frac{C \text{ moles in gas products}}{n \times \text{alcohol moles in the feedstock}} \times 100$$

The alcohols conversion to liquid products is indicated as X_L and it was calculated based on the following equation:

$$X_L = \left(\frac{\text{alcohol moles in the feedstock} - \text{alcohol moles in liquid products}}{\text{alcohol moles in the feedstock}} \right) \times 100 - X_G$$

The gas product composition [% mol/mol (dry basis)] was calculated as: produced moles of H_2 , CO , CO_2 and CH_4 respectively, divided total moles of gas phase $\times 100$. The activity on time was expressed as coefficient "a" that expresses the ratio between gaseous alcohols conversion at time "t" divided the initial gaseous alcohols conversion.

Carbon deposits were characterized by temperature programmed oxidation (TPO), measuring the weight variation as function of the temperature in a thermogravimetric instrument (Shimadzu TGA 50). Post reaction samples of 10 mg were used with air flow of $40 \text{ cm}^3 \text{ min}^{-1}$ and heating of $10^\circ\text{C min}^{-1}$ from room temperature to 850°C .

The carbon deposits were studied using Laser Raman Spectroscopy (LRS) in a LabRAM HR UV 800 (Horiba/Jobin Yvon) instrument, laser He-Ne ($\lambda = 632 \text{ nm}$), CCD detector and an OLYMPUS microscope, model BX41. The measurements of the samples, diluted in KBr, were taken with a 100x magnification and the scattered light was collected through a confocal hole of $100 \mu\text{m}$.

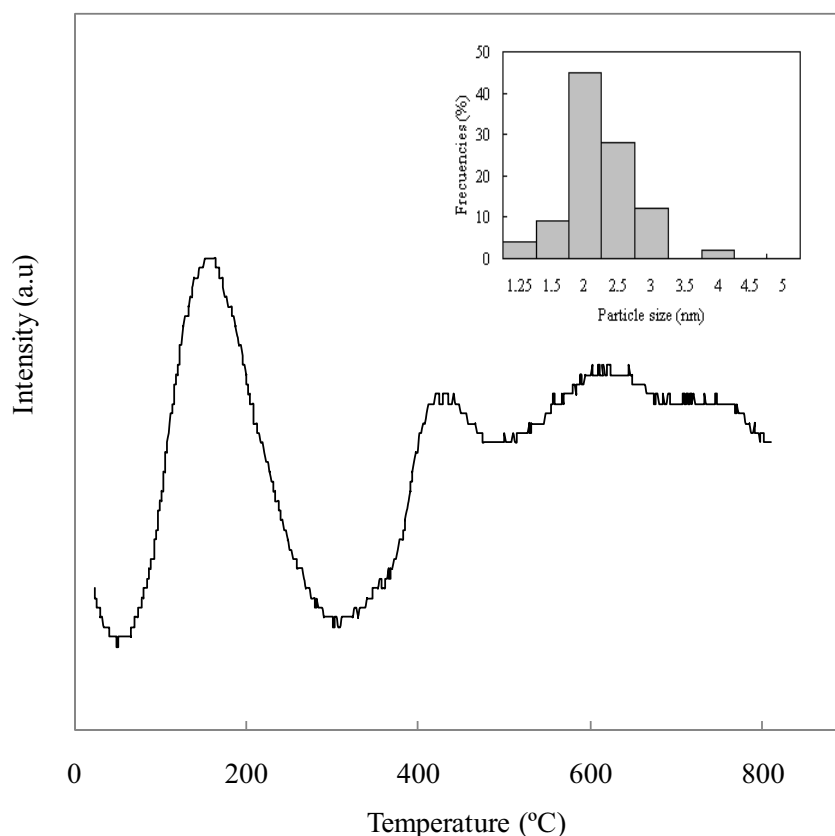
3. RESULTS AND DISCUSSION

3.1. Catalyst Characterization

Table 1 show characterization results obtained by BET, TEM, TPR, H_2 chemisorption and XPS analysis. Results of TEM measurements indicate that the particle size distribution is very narrow and centered around 2.2 nm. TPR analyses show a high reducibility degree, between 0.9 and 1. The degree of reducibility expresses the relationship between amounts of H_2 consumed respect of theoretical amount of H_2 consumption necessary to achieve the overall reduction of the oxidized species. The reducibility degree was calculated as: [(amount of H_2 consumed by TPR) / (theoretical amount of H_2 consumption for the total reduction)]. The reducibility degree is a normalized value (between 0 and 1).

Table 1. Characterization of the Studied Catalyst. Metal Content by Atomic Absorption, Mean Particle size (d_{va}) by TEM, H_2 Chemisorption (H/Pt ratio), TPR and XPS Results.

Catalyst	S_{BET} Support	wt % Pt	d_{va} (nm)	Dispersion (H/Pt)	TPR Peaks ($^{\circ}C$)		XPS ^c (eV)
		AA			LT ^a	HT ^b	Pt 4f 7/2
2PtSi ^(ie)	200	2.0	2.2	0.60	155	410	71.6

^(ie) Ionic exchange^aLT: low temperature, ^bHT: high temperature. ^c Binding energies (eV)**Fig. (1).** Temperature programmed reduction (TPR) profile. The inner figure shows the particle size distribution of reduced catalyst.

TPR profile of Pt catalyst (Fig. 1) show the existence of two main peaks of hydrogen consumption. As it was cited in the literature [11], this indicates the presence of two types of platinum oxides; with weak interaction with the support that reduces below 220 $^{\circ}C$, and with strong interaction with the support when the hydrogen consumption is from 350 $^{\circ}C$. Results of hydrogen chemisorption by the pulse method, showed that Pt catalyst have a H/Pt ratio of 0.6, indicating a high metallic dispersion. As regards the XPS analysis, the value at 71.6 eV of level Pt 4f $_{7/2}$ is reported in Table 1, indicating the complete reduction of platinum.

3.2. Steam Reforming Reactions

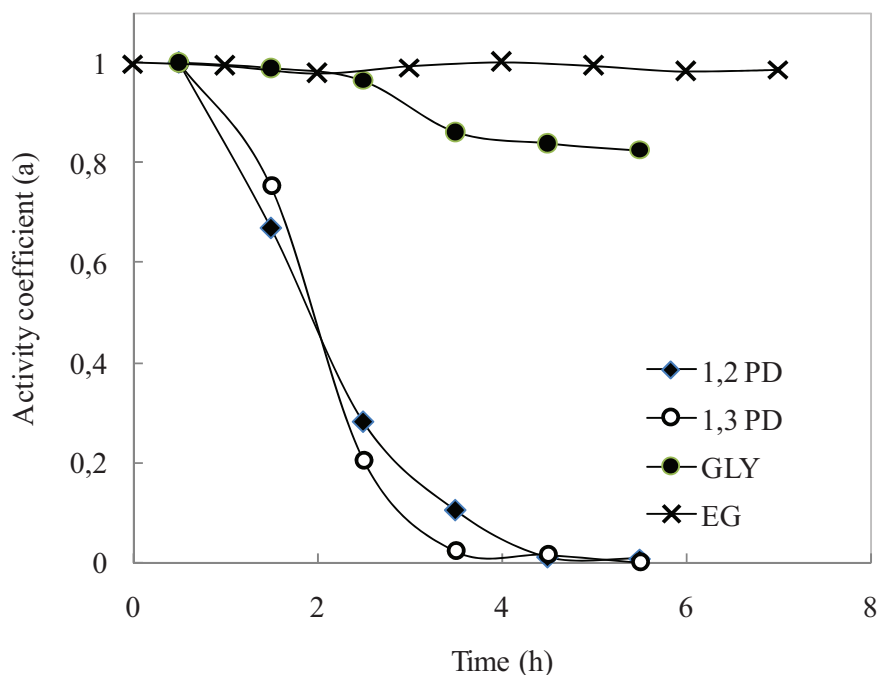
Steam reforming reactions of C3 alcohols (1-propanol, 2-propanol, 1,2-propanediol, 1,3 propanediol, and glycerol) were studied under conditions previously indicated in the experimental section. The space time (τ) employed in order

to be able to determine the presence of reaction intermediates was 0.88 min. Table 2 shows the results of steam reforming of the different C3 alcohols, displaying the conversion to: gaseous products (X_G), liquid products (X_L) and the gaseous products distribution calculated on dry basis. It is observed that the reactivity of the alcohols in these reaction conditions follows the order: glycerol > 1,2-propanediol > 1,3-propanediol > 2-propanol > 1-propanol. Higher conversions to gaseous products were obtained with glycerol (GLY), 1,2-propanediol (1,2 PD) and 1,3-propanediol (1,3 PD). With 1-propanol (1P) and 2-propanol (2P) conversion to gaseous products was very low, around 1%, and remained very low even at 650 $^{\circ}C$ with 2P. This indicates that the presence of polyols functions increases the yield to gases.

Fig. (2) shows the evolution of catalytic activity on time on stream of 1,2 PD, 1,3 PD, EG and GLY defined as coefficient “a” that expresses the ratio between gaseous alcohols conversion at time “t” divided the initial gaseous alcohols

Table 2. Alcohols Conversion and Gaseous Products Distribution in the Steam Reforming (Data Collected after 2 h of Operation).

Reagent	Temp (°C)	X_G (%)	X_L (%)	% mol/mol dry basis			
				H ₂	CO	CH ₄	CO ₂
1-Propanol	350	1	4	70	21	8	1
	650	37	1.5	72	6.6	3.7	18
2-Propanol	350	<1	21	65	32	2	1
	650	1.4	11	85	5	0.7	28
1,3-Propanediol	350	35	13	48	37	11	4
	450	57	17	48	30	15	7
1,2-Propanediol	350	32	43	49	36	14	1
	450	76	20	45	35	16	4
Glycerol	350	85	3	57	40	1	2
	450	100	0	62	27	10	1

**Fig. (2).** Activity results of steam reforming of 1,2-propanediol (1,2 PD), 1,3-propanediol (1,3 PD), glycerol (GLY) and ethylene glycol (EG) versus time on stream at 450°C and $\tau = 0.88$ min.

conversion. It is observed a significant loss of coefficient "a" in 1,2 PD and 1,3 PD while the activity of GLY and EG decreases slightly.

3.2.1. Steam reforming of 1-Propanol (1P) and 2-Propanol (2P)

As it can be seen in Table 3 the main products to 1P and 2P are propanal and 2-propanone respectively. These are the first intermediate that appears in dehydrogenation reactions

and also can be appreciated that do not occur subsequent C-C bond cleavage reactions (Fig. 3). The results indicate that the dehydrogenation step is more favorable for 2P ($X_L = 21\%$), which may relate to the OH group bonding to a secondary carbon [12]. These points out the differences in reactivities between a primary and a secondary alcohol function. Furthermore, some authors report the differences in the adsorption force of aldehydes and ketones [13]. Thus, propanal absorption is stronger than the acetone, inhibiting the activity of the catalyst (Fig. 2).

Table 3. Liquid Phase Product Distribution as a Function of Reaction Temperature.

Reagent	Temp (°C)	X _L (%)	Products Identified in Liquid Phase	% mol/mol
1-Propanol	350	4	Propanal	97
	650	1,5	Propanal	27
2-Propanol	350	21	Acetone	98
	650	11	Acetone	70
1,3 Propanediol	350	13	Acetaldehyde	23
			Ethanol	73
	450	17	Acetaldehyde	12
			Ethanol	88
1,2 Propanediol	350	43	1-hydroxy-2-propanone (acetol)	38
			2,3-Epoxy-1-propanol (glycidol)	31
			2-hydroxypropanal	29
			2-oxopropanal	1
	450	20	1-hydroxy-2-propanone (acetol)	14
			2,3-Epoxy-1-propanol (glycidol)	17
			1-propanol	4
			2-oxopropanal	64
Glycerol	350	3	1,3-dihydroxy- 2-propanone	27
			1-hydroxy-2-propanone (acetol)	12
			2-oxopropanal	19
			2,3-dihydroxypropanal	6
			1,2 ethanediol (ethylene glycol)	7
			2-hydroxyethanal	23

3.2.2. Steam reforming of 1,2 Propanediol (1,2 PD) and 1,3 Propanediol (1,3 PD)

Comparing the results obtained for 1,3 PD and 1,2 PD it can be seen that the conversion to gaseous products are similar (35 vs. 32% respectively), however, the differences are observed in the conversion to liquid products (Table 2).

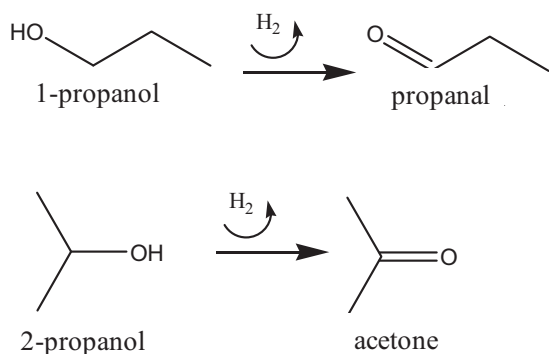


Fig. (3). Dehydrogenation reaction scheme for 1-propanol (1P) and 2-propanol (2P).

The higher conversion to liquid products at 350°C is achieved with 1,2 PD (X_L = 43%). The main liquids products of 1,2 PD were: 1-hydroxy-2-propanone (acetol) > 2,3-Epoxy-1-propanol (glycidol) > 2-hydroxypropanal > 2-oxopropanal. These results allow proposing the reaction scheme shown in Fig. (4). According to this scheme, consecutive dehydrogenation reactions lead to 2-oxopropanal and the subsequent C-C bonds cleavage lead to the formation of CO and CH₄, and this would be the primary route of gas production. The absence of acetone indicates that the C-O bonds cleavage reactions do not occur. In a first step and due to keto-enol tautomerism, acetol can interconverted into its enol form and subsequently by epoxidation reaction glycidol is obtained. It is well known the tendency of glycidol to polymerize, allowing to explain the strong deactivation observed in Fig. (2). It can be observed a marked increase in the conversion to gaseous products when the temperature is increased to 450°C (Table 2) as well as the increasing in the content of 2-oxopropanal (Table 3), these results allow to establish that 2-oxopropanal represents a major intermediate for gas production (Fig. 4).

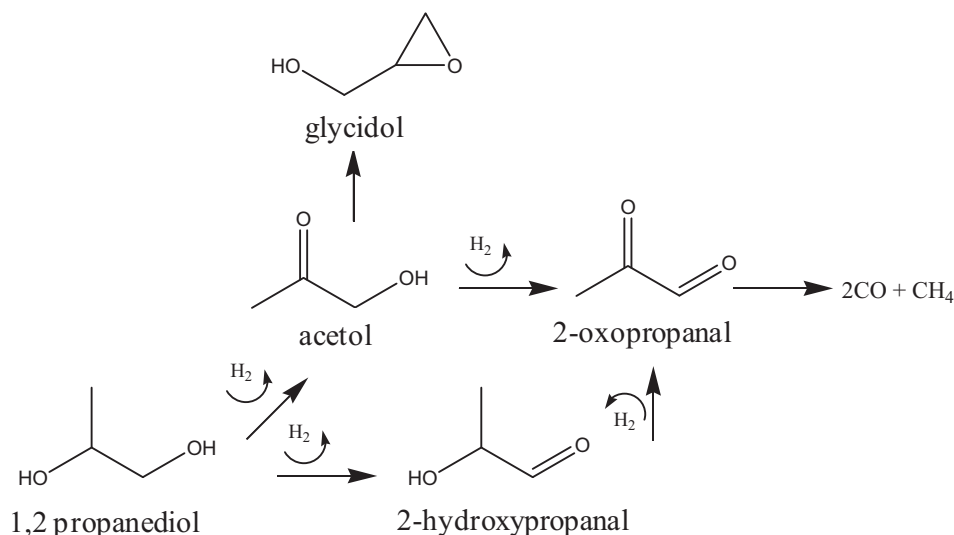


Fig. (4). Dehydrogenation reaction scheme for 1,2 Propanediol (1,2 PD).

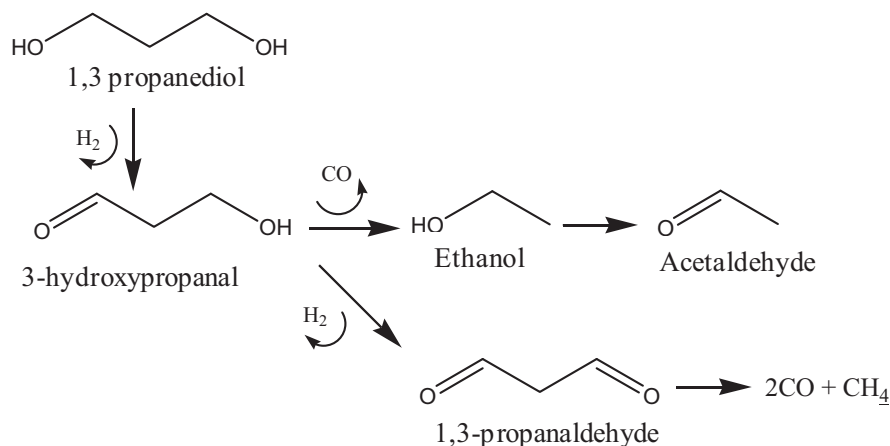


Fig. (5). Dehydrogenation reaction scheme for 1,3 Propanediol (1,3 PD).

Conversion to liquid products for 1,3 PD was 13% at 350°C and the mainly compounds identified were ethanol and acetaldehyde. In the same way that the presence of propanal inhibits the dehydrogenation of 1P, the strong surface adsorption of acetaldehyde reduces the catalyst activity. The reactions involved could be the proposed at the scheme of Fig. (5).

3.2.3. Steam Reforming of Glycerol

We have previously determined that in the steam reforming of glycerol the main intermediaries were 1,3-dihydroxy-2-propanone and 2,3-dihydroxypropanal [8]. The reaction pathways for H_2 production by steam reforming of glycerol is shown in Fig. (6). Starting from this point, two reaction pathways can occur, indicated in Fig. (6) as [I] or [II]. The pathway [I] would indicate that due to a first dehydration step 1-hydroxy-2-propanone (acetol) is obtained, that by a subsequent dehydrogenation leads to 2-oxopropanal. From this point, the cleavage step of C-C and C-O bonds would begin. The pathway [II] does not involve dehydration reactions, but it involves mainly cleavage of C-C bonds and dehydrogenations, producing H_2 and CO. Is worth recalling

that the results obtained for simple alcohols show aldehydes as reaction intermediates (propanal, acetaldehyde), while in the glycerol reforming was determined the presence of hydroxyaldehydes. According to our results, the smallest presence of intermediate 2,3-dihydroxypropanal in reaction products could indicate the highest relative rate of reactions of pathway [II]. The low production of CO_2 and CH_4 could be attributed to the low contribution of pathway [I], water gas shift and methanation reactions at low space times. The presence of acetol would indicate that 1,3-dihydroxy-2-propanone undergoes rupture reactions of C-O bonding. However, due to the low content of CH_4 , it is possible to establish that the rupture of C-C bond predominate over the C-O bond cleavage. Therefore the main path leading up to gaseous products involve the C-C rupture reactions on primary alcohols such as 2,3-dihydroxypropanal, 1,2-ethanediol and hydroxyacetaldehyde (Fig. 6).

3.2.4. Steam Reforming of Acetol (AC) and Ethylene Glycol (EG)

In order to confirm the proposed reaction pathways for glycerol, steam reforming of ethylene glycol (1,2 ethanediol)

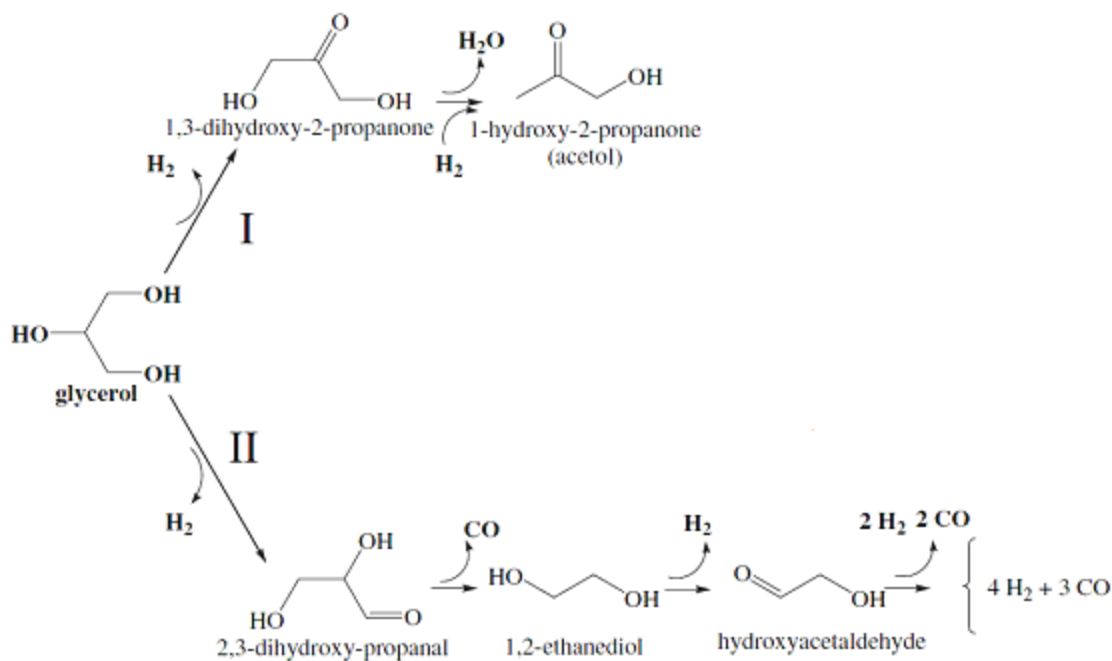


Fig. (6). Reaction pathways for H_2 production by steam reforming of glycerol [8].

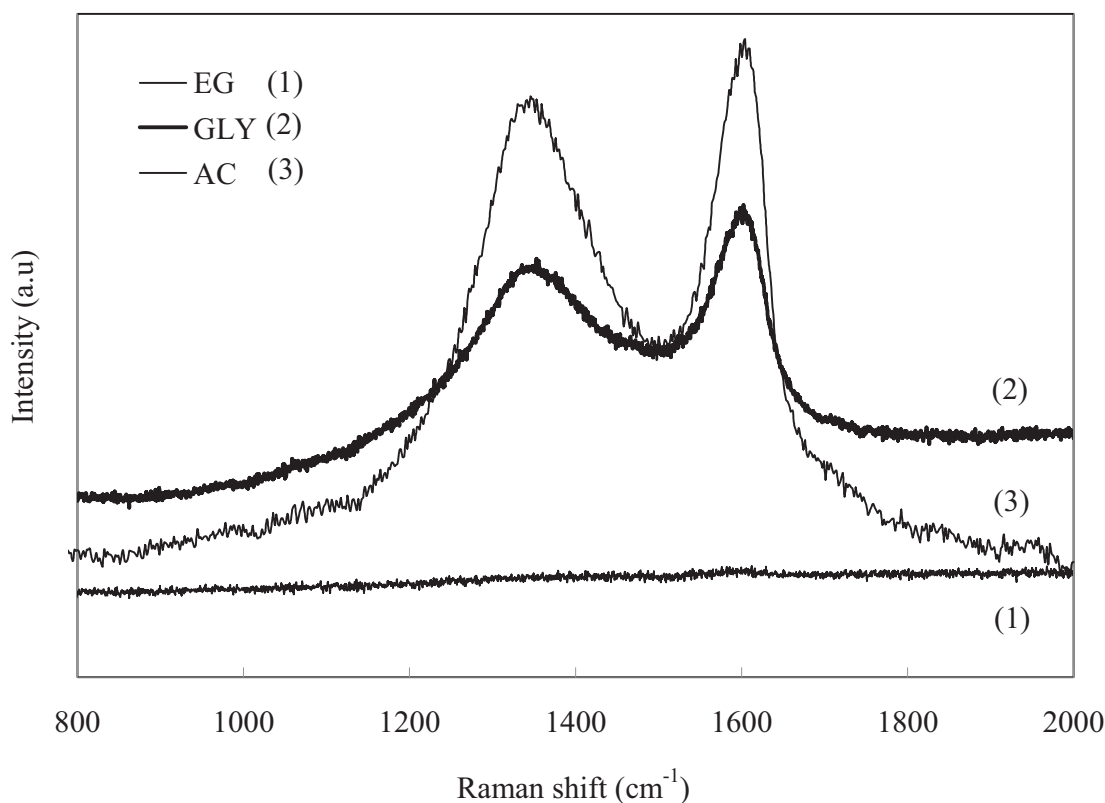


Fig. (7). Raman spectra of carbon species formed after steam reforming of glycerol (GLY), acetol (AC) and ethylene glycol (EG) at 450°C.

and 1-hydroxy-2-propanone (acetol) were carried out. The obtained results show that in the steam reforming of EG the conversion to gaseous products was 70%, with a H_2/CO molar ratio of 1.6, very close to the theoretical ratio of decomposition (1.5). EG conversion to liquid products was 12%,

being methanol and 2-hydroxyethanal the major products identified in liquid phase.

Furthermore, the AC steam reforming show a very low conversion to gaseous products (5%) while the conversion to

liquid products was 95%, glycidol (coming from side reactions of AC) and polyethylene glycols of higher molecular weight were identified in liquid phase. In contrast to EG, AC reforming shows a very fast deactivation due to the tendency of the glycidol to be polymerized.

3.3 Carbon Deposition

The TPO/TGA analyses allowed determination of deposited carbon. Comparing the post-steam reforming reaction samples of 1,2 PD and 1,3 PD it can be seen that the 1,3 PD had a higher carbon content than 1,2 PD sample (1,7% wt vs. 1,3% wt) which is consistent with the rapid deactivation observed during the steam reforming reaction (Fig. 2). From TGA/TPO analysis of 1,3 PD sample, two peaks are observed (not shown), the first one at 300°C (weight loss of 1% wt) and the second one with a weight loss of 0.7% wt at 500°C. The first peak could be assigned to amorphous carbon of low-interaction, while the carbon deposit burned at 500°C has more interaction and more ordered structure. Sample 1,3 PD has the highest acetaldehyde content, therefore, it can be concluded that acetaldehyde is the precursor of carbon burned at low temperature (300°C), while for 1,2 PD sample acetol and glycidol appear to be the carbon precursors.

Comparing the EG and GLY carbon content on post-steam reforming reaction samples (after 24 hours of time on stream) is observed that in the EG posreaction sample the carbon content is very low (0.6 %wt, burning temperature 500°C.) which is consistent with the excellent stability over time (Fig. 2). Furthermore, the GLY post-steam reforming sample has higher carbon content (2% wt) with the burning temperature 500°C.

The carbon deposits were studied by laser Raman spectroscopy (LRS), a widely used technique in the analysis of crystalline, nanocrystalline and amorphous carbon. The tangential-mode G band appearing in the 1400-1700 cm^{-1} region is related to the Raman-allowed phonon mode E_{2g} and involves out-of-phase intralayer displacement in the graphene structure. It provides information about the electronic properties and is a measure of the presence of ordered carbon. The so-called D band at around 1350 cm^{-1} is related to defects or the presence of nanoparticles and amorphous carbon [14]. The D and D' bands (refers to the A_{2g} mode due to the breathing mode of sixfold ring), at 1360 and 1610 cm^{-1} respectively are assigned to amorphous carbon and the band G (related to the stretching vibration mode E_{2g} in $\text{C}=\text{C}$ (C sp^2) bond) at 1580 cm^{-1} correspond to graphitic carbon [15]. Fig. (7) shows the result of Raman spectra of carbon species formed after steam reforming of GLY, AC and EG at 450°C. One can observe that in the catalysts used in the steam reforming of AC and GLY the Raman signals appearing at 1360 and 1610 cm^{-1} are typical of the non-crystalline carbon deposits. This is evidence that the AC is the main intermediary which causes the formation of coke and subsequent deactivation.

4. CONCLUSIONS

The results obtained allowed to establish:

1. The absence of C-O and C-C bond cleavage in a secondary alcohol.
2. The presence of reaction intermediates with aldehyde function deactivates the catalyst due to the strong adsorption on the metal sites, moreover, the presence of hydroxyl-aldehydes promote the C-C bonds cleavage favoring the gas production pathway.
3. The reaction pathway from glycerol to acetol by cleavage C-O bonding or dehydration on metal site is responsible for the subsequent reactions leading to deactivation.
4. The main reaction pathway to obtain gaseous products from glycerol reforming involve C-C bonds cleavage of primary alcohols such as 2,3-dihydroxypropanal to obtain ethylene glycol.

CONFLICT OF INTEREST

The authors confirm that this article content has no conflicts of interest.

ACKNOWLEDGEMENTS

We thank the financial support from ANPCyT PICT N° 1962, Project I175 UNLP and CONICET PIP 542.

REFERENCES

- [1] Montini, T.; Singh, R.; Das, P.; Lorenzut, B.; Bertero, N.; Benedetti, P.; Giambastiani, G.; Bianchini, C.; Zinoviev, S.; Mier-tus, S.; Fornasiero, P. Renewable H_2 from Glycerol Steam Reforming: Effect of La_2O_3 and CeO_2 Addition to $\text{Pt}/\text{Al}_2\text{O}_3$ catalysts. *Chem.Sus.Chem.*, **2010**, *3*, 619-628.
- [2] Luo, N.; Zhao, X.; Cao, F.; Xiao, T.; Fang, D. Thermodynamic Study on Hydrogen Generation from Different Glycerol Reforming Processes. *Energy & Fuels*, **2007**, *21*, 3505-3512.
- [3] Iriondo, A.; Barrio, V.; Cambra, J.; Aria, P.; Guemez, M.; Sanchez-Sanchez, M.; Navarro, R.; Fierro, J. Glycerol steam reforming over Ni catalysts supported on ceria and ceria-promoted alumina. *Int. J. Hydrogen Energy*, **2010**, *35*, 11622-11633.
- [4] Iriondo, A.; Guemez, M.; Barrio, V.; Cambra, J.; Aria, P.; Sanchez-Sanchez, M.; Navarro, R.; Fierro, J. Glycerol conversion into H_2 by steam reforming over Ni and PtNi catalysts supported on MgO modified Al_2O_3 . *Stud. Surf. Sci. Catal.*, **2010**, *175*, 449-452.
- [5] Iriondo, A.; Barrio, V.; Cambra, J.; Aria, P.; Guemez, M.; Sanchez-Sanchez, M.; Navarro, R.; Fierro, J. Influence of La_2O_3 modified support and Ni and Pt active phases on glycerol steam reforming to produce hydrogen. *Catal. Comm.*, **2009**, *10*, 1275-1278.
- [6] Soares, R.; Simonetti, D.; Dumesic, J. Glycerol as a Source for Fuels and Chemicals by Low-Temperature Catalytic Processing. *Angew. Chem., Int. Ed.*, **2006**, *45*, 3982-3985.
- [7] Shabaker, J.; Huber, G.; Davda, R.; Cortright, R.; Dumesic, J. Aqueous-Phase Reforming of Ethylene Glycol over Supported Platinum Catalysts. *Catal. Lett.*, **2003**, *88*, 1-8.
- [8] Pompeo, F.; Santori, G.; Nichio, N. Hydrogen and/or syngas from steam reforming of glycerol. Study of platinum catalysts. *Int. J. Hydrogen Energy*, **2010**, *35*, 8912-8920.
- [9] Pompeo, F.; Santori, G.; Nichio, N. Hydrogen production by glycerol steam reforming with Pt/SiO₂ and Ni/SiO₂ Catalysts. *Catal. Today*, **2011**, *172*, 183- 188.
- [10] Simonetti, D.; Kunkes, E.; Dumesic, J. Gas-phase conversion of glycerol to synthesis gas over carbon-supported platinum and platinum-rhenium catalysts. *J.Catal.*, **2007**, *247*, 298-306.
- [11] Merlen, E.; Beccat, P.; Bertolini, J.; Delichere, F.; Zanier, N.; Didillon, B. Characterization of Bimetallic Pt-Sn/ Al_2O_3 Catalysts: Relationship between Particle Size and Structure. *J.Catal.*, **1996**, *159*, 178.

- [12] Xun, H.; Gongxuan, L. Investigation of the Effects of Molecular Structure on Oxygenated Hydrocarbon Steam Re-forming. *Energy & Fuels*, **2009**, *23*, 926–933.
- [13] van Druten, G.; Poncet, V. Hydrogenation of carbonylic compounds: Part I: Competitive hydrogenation of propanal and acetone over noble metal catalysts. *Appl. Catal. A*, **2000**, *191*, 153–162.
- [14] Saito, R.; Takeya, T.; Kimura, T.; Dresselhaus, G.; Dresselhaus, M. Electronic structure of graphene tubules based on C60. *Phys. Rev. B*, **1992**, *46*, 1804.
- [15] Pimenta, M.; Jorio, A.; Brown, S.; Souza, F.A.; Dresselhaus, G.; Hafner, J.; Lieber, C.; Saito, R.; Dresselhaus, M. Diameter dependence of the Raman D-band in isolated single-wall carbon nanotubes. *Phys. Rev. B*, **2001**, *64*, 41401R.

Received: June 06, 2013

Revised: December 12, 2013

Accepted: December 17, 2013